Enhanced Confinement and Stability of a Field-Reversed Configuration with Rotating Magnetic Field Current Drive

J. T. Slough and K. E. Miller

Redmond Plasma Physics Laboratory, University of Washington, Seattle, Washington 98195

(Received 15 February 2000)

A new experiment has been constructed to study the sustainment of a field-reversed configuration (FRC) with a rotating magnetic field (RMF). FRCs were formed with cold, unmagnetized ions and thus without a kinetic ion component that was believed to provide stability to internal tilt modes. No destructive instabilities were observed for the RMF FRC. Only peripheral radial penetration of the RMF was observed. The radially inward flow arising from axial screening currents at the FRC edge reduced convective and conductive losses to the measurement limit of the diagnostics.

PACS numbers: 52.55.Hc, 52.55.Dy

Fusion research has focused on the tokamak concept which has resulted in large, expensive reactor designs. This dictates exploring novel, simpler, and less costly configurations. A leading candidate is the field-reversed configuration (FRC), a compact toroidal geometry, which has the geometrically simplest, most compact, and highest β of all magnetic fusion confinement schemes [1,2]. It has also been recognized that the linear geometry, high plasma β, and linear exhaust of the FRC make it the ideal candidate for space propulsion applications [3].

FRCs have previously been made in a high-voltage, pulsed device called a field-reversed theta pinch (FRTP). Results from previous FRC experiments indicated confinement scaling that could lead to fusion [4], but it was also clear that the FRTP initiation method would not provide the closed flux required for a reactor. There was a method that had been investigated for years that generated the toroidal currents directly by means of a transverse rotating magnetic field (RMF) as illustrated in Fig. 1 [5–7]. Past experiments have been limited to currents of only a few kA, so that the confining axial magnetic field generated was no larger than the RMF. The effects of the RMF on the FRC plasma confinement were also unknown as the plasmas generated in these experiments were partially ionized and in contact with the vessel wall.

A new experiment, the Star Thrust Experiment (STX) [3], was constructed of a size and power such that the axial field swing ΔB_z (200 G), produced by the RMF field, was much larger than the RMF field B_ω (20 G) used to generate it. The FRC was also formed in a flux-conserving coil [1] and operated in a manner that prevented FRC contact with the vacuum vessel wall. STX was also designed so that the FRC could be produced in the conventional manner (FRTP). In this way, the possibility of sustaining a preexisting FRC could also be investigated, as well as obtain a measure of the influence of the RMF on the decaying FRC.

When applied to a plasma embedded with a constant axial magnetic field in a flux conserving coil, the RMF drives a strong azimuthal current that reverses the direction of the initial magnetic field, and produces the field-reversed configuration. Unlike FRTP formation, where this current is driven by an induced azimuthal voltage caused by rapid field reversal, the RMF current is driven in an inherently steady state manner which allows for the sustainment of the configuration. A starting point for understanding the current drive process is the generalized Ohm's Law, where it will be assumed for the moment that the ions form a fixed uniform background (the $\mathbf{u} \times \mathbf{B}$ term is ignored):

$$\mathbf{E} + (\mathbf{u} \times \mathbf{B}) = \eta \mathbf{j} + \mathbf{j} \times \mathbf{B}/ne = \eta[\mathbf{j} + (\omega_{ce}/\nu_{ei})\mathbf{j} \times \mathbf{e_B}], \quad (1)$$

where B has oscillating components in the θ and r directions due to the RMF at a frequency ω_{RMF}, and a steady axial field provided by the axial field coils. If the Hall term $\mathbf{j} \times \mathbf{B}/ne$ is small compared to the resistive term, $E_\theta = \eta j_\theta$ is positive, and from Faraday's law, $d\phi/dt$ is negative and the FRC decays. With the Hall term dominant, E_θ, for sufficiently small η or large $\langle j_z B_r \rangle$, can be negative with a subsequent increase in flux.

A requirement on the RMF is that it penetrate the plasma. The solution of Ohm's law, neglecting the Hall term, is characterized by the RMF penetrating a distance $\delta = (2\eta/\omega\mu_0)^{1/2}$, which is the resistive skin depth for a conductor in an rf field. However, the regime of

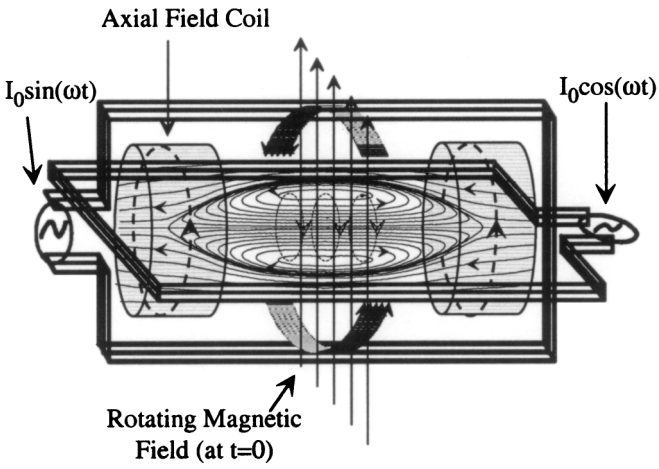

FIG. 1. RMF current drive in a cylindrical flux-conserving coil.

 0031-9007/00/85(7)/1444(4)$15.00

interest here is a plasma where $\nu_{ei} \ll \omega_{ce}$ (so that the electrons stay magnetized to the RMF). In this limit, from Ohm's law, $j_\theta \approx -ner\omega$ and $j_z \approx E_z/(\eta\omega_{ce}{}^2/2\nu_{ei}{}^2)$ [5]. The electrons are in synchronous rotation with the RMF, and their response to the axial electric field is severely restricted (small j_z), and unable to screen out the RMF field. From another viewpoint, the corotating electrons experience a nearly steady transverse field, and the effective field penetration can be many times the resistive skin depth. One can define two dimensionless parameters that describe the RMF penetration condition.

$$\gamma_\omega = \frac{\omega_{ce}}{\nu_{ei}}, \qquad \lambda = \frac{R}{\delta}. \tag{2}$$

Penetration can be maintained as long as $\gamma_\omega > \lambda$ [8,9].

The Hall term has two pondermotive components: the $\langle j_z B_r \rangle$ term acting in the θ direction and the $\langle j_z B_\theta \rangle$ term acting in the r direction. Since j_z, B_r, and B_θ vary in time at the frequency ω_{RMF}, both the pondermotive forces in r and θ directions have a steady part. From the $\langle j_z B_r \rangle$ force, the electron fluid will attain that steady value of azimuthal velocity that corresponds to the balancing of the steady accelerating torque by the retarding torque (due to electron–ion collisions). In this way a steady azimuthal current density,

$$j_\theta = -ne\omega_{\mathrm{RMF}} r, \tag{3}$$

is produced. Since the RMF field was observed to penetrate only to the field null, these pondermotive forces acted only at the outer edge of the FRC. The effect of large plasma screening currents (j_z) allows for the radially acting $\langle j_z B_\theta \rangle$ force to produce a radially inward pressure at the plasma edge. In equilibrium ($E_\theta \sim 0$), the larger $\langle j_z B_r \rangle$ term must now be balanced by $u_r B_z$ and the flow term in Eq. (1) cannot be ignored. To achieve equilibrium inside the FRC, where there is no RMF, the axial field pressure must be balanced by a radial inward plasma flow as well. This flow was manifested experimentally by the radially inward displacement of the plasma pressure profile. The flow and radial profile changes have been observed in recent resistive 2D MHD calculations of the RMF driven plasma [10], with profiles that are identical to those found in the experiment. This induced flow opposes the radially outward flow from plasma diffusion and would thus inhibit particle loss at the separatrix.

The STX chamber consisted of a 3-m-long, 20.5-cm inner radius quartz vacuum tube that was surrounded by 8 parallel-fed, four-turn solenoidal coils at a radius of 23 cm. The coils provided a flux-preserving axial field that prevented plasma wall contact during RMF current ramp-up.

The RMF is generated by two mutually perpendicular coils driven 90° out of phase. In order to drive the RMF antennas, two power supplies, capable of delivering several megawatts for the duration of the experiment, were employed in order to rapidly ionize and heat the plasma. Details of the RMF antenna system are given elsewhere [3,11].

Because of the pulsed nature of the power supplies, the time that the flux could be held constant on the main pinch coil was limited to roughly 0.5 ms. This, however, was sufficient to establish an equilibrium condition and gain information about the power input and losses from the FRC. The formation sequence employed in the discharge of Fig. 2 was to first form an FRC via the FRTP method. The initial FRC decayed away rapidly. Out of the remnant plasma, the RMF was applied at 0.1 ms and rapidly restored the toroidal current and reformed the FRC. A plot of the internal field structure for both the initial and RMF FRC is shown in Fig. 3. This data was obtained from a radial array of internal magnetic probes that recorded both the axial and azimuthal internal field components.

If the RMF was applied immediately after field reversal, the initial FRC turbulence died away and field reversal was never lost. A Langmuir triple probe was used to monitor the plasma flow in the end region axially outside the FRC. The end flow increases steadily during the decay of the initial FRTP FRC. It is not until the RMF FRC is established that the end flow is reduced to near zero [12]. It was observed in both the RMF MHD calculations [10] as well as the experiment that the plasma density near the separatrix was quite small [12]. The dramatic decrease in separatrix pressure for the RMF driven FRC compared to the early FRTP FRC is readily observed in Fig. 3(b). With the RMF induced reduction in pressure near the separatrix,

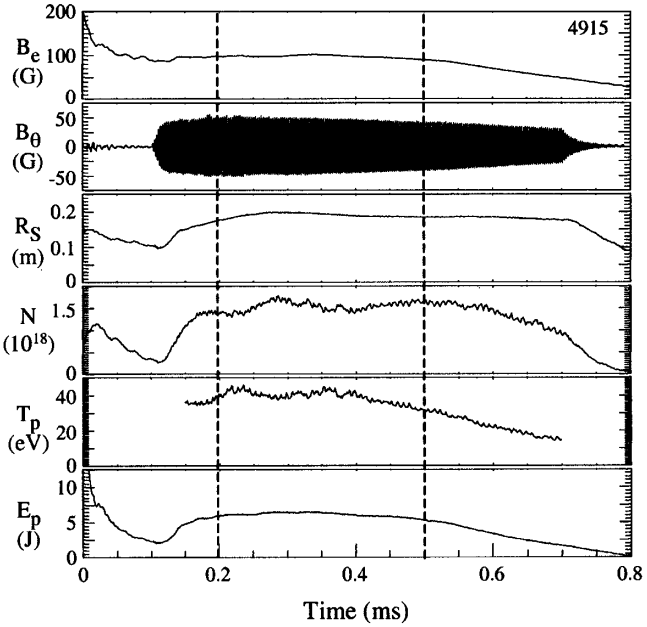

FIG. 2. Time history for various plasma parameters during a discharge. B_e is the external axial magnetic field, B_θ is the azimuthal component of the RMF field, R_s is the FRC separatrix radius, N is the FRC particle inventory, T_p is the pressure balance temperature at the magnetic null, and E_p is the FRC energy. Dashed lines indicate the time frame that quasisteady conditions were maintained.

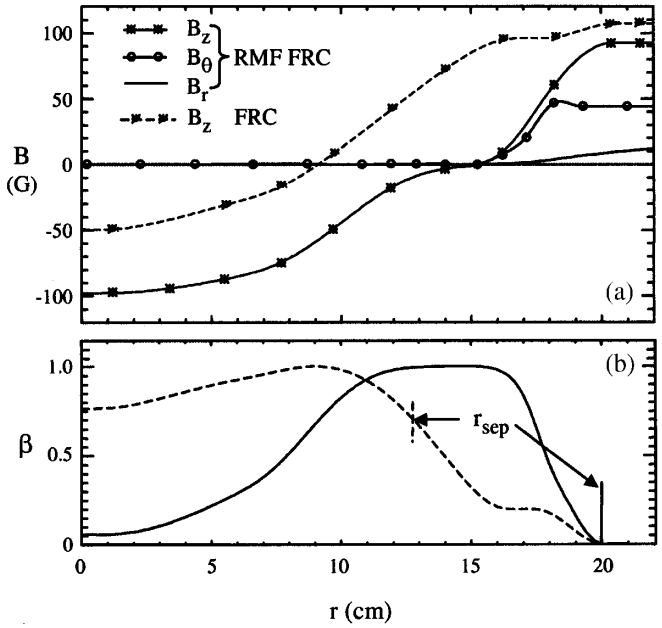

FIG. 3. (a) Internal magnetic field radial profiles at $t = 0.04$ ms (FRC) and 0.3 ms (RMF FRC). B_z is the measured steady axial field, B_θ is the measured peak azimuthal RMF field, and B_r is the inferred peak radial RMF field. (b) β determined from the magnetic profiles in (a) where β is defined here as the local plasma pressure divided by the radial magnetic pressure at the coil wall. The separatrix position R_{sep} is determined by integrating the axial field radially outward until $\psi = 0$. The dashed curves indicate values obtained from the initial "conventional" FRC formed without the RMF field.

the pressure along the inner flux surface near the axis of symmetry was near zero as well. The β at the separatrix, β_s, to within the accuracy of the field measurements ($\sim$5%) was a few percent. The conventional start-up FRC, however, showed the usual high $\beta_s \sim 0.7$ [Fig. 3(b)]. One would expect that this reduction in pressure at the separatrix should lead to considerable enhancement of the FRC particle confinement. The very flat magnetic profile stretched inward, as well as the very low separatrix beta, was also seen in the 2D MHD calculations where strong radial flow was present.

From Fig. 2 it can be seen that the FRC separatrix radius, energy, and particle inventory remained essentially constant during the time the coil flux could be held constant. These quantities were evaluated in the usual way for the FRC geometry [1]. The experiments were performed at an RMF frequency $\omega = 2.2 \times 10^6$ rad/sec, and at an average RMF vacuum field $B_\omega = 20$ G. The average density at a radius of 14 cm was found from axial interferometry to be $\sim 5 \times 10^{18}$ m^{-3}. Using the measured ion temperature from Doppler broadening, $T_i \sim 2$–3 eV, the inferred STX electron temperature from pressure balance at the null yields $T_{e0} \sim 40$ eV. The low ion temperature is not characteristic of the usual FRC experiments, but due to the low density of these discharges, charge exchange losses kept the deuteron ion energy to that acquired during dissociation. Unlike previous FRC experiments, it was possible to independently determine the plasma density and temperature at the plasma edge since the current density, and thus electron density [see Eq. (3)] is known from the magnetic profile [see Fig. 3(a)]. The local temperature can then be determined from radial pressure balance. It was found to be somewhat higher ($\sim$60 eV) than the axial line average inferred from interferometry at the null. Since there was little current density (joule heating) and maximum density at the null, radiative cooling may dominate the heat flow from the low density, joule heated plasma edge.

With these conditions a $\lambda \approx 65$, with a $\gamma_\omega = 375$, are inferred at the FRC null. These values are well above critical level, and the RMF field would be expected to fully penetrate the plasma. From previous analysis [8,9], the RMF must diffuse radially inward into the FRC to drive current. The time scale for penetration into 40 eV plasma of radius $R \sim 19$ cm as in Fig. 3 would be $\sim$0.6 ms. The actual penetration time was observed to be as rapid as 0.05 ms, indicating that the resistivity of the initial decaying FRC is large (the electron temperature determined from the triple probe is less than 15 eV at this time). It can be seen in Fig. 3 that a large radial RMF at the null was not required to drive current or reverse the axial magnetic field deep within the FRC. The current driven radially inside the magnetic null is a consequence of pressure equilibration along flux surfaces, i.e., $P = P(\psi)$.

The lack of deeper penetration may be explained by either an equilibrium profile constraint, a lack of sufficient time for penetration as the plasma temperature near the edge rapidly increases, or an anomalously high resistivity near the FRC null preventing further penetration. After the RMF FRC is formed, the RMF field was observed to move farther out from the FRC null as the FRC radius decayed, and repenetration was not typically observed. The possibility of ion corotation as the mechanism for the slow flux decay was not likely due to the long ion-electron equilibration time (many milliseconds). No Doppler shift was observed in the deuterium line emission along a chord near the FRC edge during the discharge as well.

A global measure of the plasma resistivity can be obtained from power balance. During the equilibrium period where plasma conditions are nearly constant, the only energy input to the plasma is from the RMF antennas in the form of the ηj_θ^2 heating of the plasma. It was determined that the capacitor bank energy not accounted for by circuit losses was 30 J from 0.2 to 0.7 ms (when the RMF was turned off). It was not possible to observe any plasma loading losses from the antennas during the discharge so that no detailed temporal information could be ascertained about the power flow during the equilibrium. The average power input into the plasma, however, can be determined during this time and was $\sim$60 kW with an uncertainty of $\pm$30 kW. Since the FRC energy remains constant during the equilibrium period, the total power lost from the FRC must be of the same order as the input.

Given the current density profile, derived from the magnetic field profiles shown in Fig. 3(a), along with the

average temperature inferred from pressure balance ($T_e \sim T_p \sim 40$ eV), one would expect ~40 kW of classical resistive heating from the axial and azimuthal currents. This would indicate a near classical resistivity where the currents are driven. The Ohmic heating of the electrons is balanced by thermal conduction losses, P_{ce}, radiation losses, P_{rad}, and particle loss P_N. Since the ions are observed to be cold, there is also an additional power lost to equilibration with the ions, $P_{ei} \sim 6$ kW. From previous FRC experiments [2], the major impurities are carbon and oxygen. The radiation losses were estimated from doping the deuterium fill gas with CO_2. This method is appropriate at these plasma densities because the impurity radiation is relatively insensitive to electron temperature [13]. Doping at 0.5% roughly doubled the radiation level and caused a major degradation in the RMF current drive. This would be expected, as the power lost through radiation was a major loss channel in STX with the inferred radiative power loss $P_{\mathrm{rad}} \sim 14$ kW. Because of the low plasma density near the separatrix, only convective particle losses are assumed since the mean free path for the electrons is tens of meters. The high FRC edge temperature also supports the assumption of small thermal conduction losses.

Assigning all the remaining power loss to the convective power loss, a lower bound for the RMF FRC particle confinement can be made. The energy and particle inventory were observed to not decay during the equilibrium period denoted by dashed lines in Fig. 2. Thus each electron-ion pair that was lost was replaced, most likely through charge exchange, and heated to the bulk FRC temperature. The energy loss from particle loss is $\frac{5}{2}kT_p$ per pair, reflecting both the particle kinetic energy loss as well as the work done on the external field. There is also ionization losses of at least ~25 eV per pair. Setting this equal to the 40 kW of the remaining Ohmic power, a particle confinement $\tau_N = 1.3$ ms is inferred. Since no thermal conduction losses were assumed, this should represent a worst-case estimate. The energy confinement time considering only conductive and particle losses was 0.2 ms. The confinement without the RMF could be obtained by turning off the RMF at various times in the equilibrium phase. The FRC energy and particles decay on a much more rapid time scale with $\sim\tau_E = 0.04$ ms, close to the predicted confinement based on scaling laws obtained from previous FRC experiments [1,4]. The FRC confinement was thus substantially improved by the application of the RMF field. The particle confinement was found to be as good as or better than that observed in even the largest FRC experiments performed previously at much higher confining fields.

Since the ratio of the ion gyrofrequency to ion collision frequency $\sim 0.04 \ll 1$, the ions are essentially unmagnetized due to the low ion temperature. Thus, for the first time, the FRC produced in these experiments was in a regime where the stabilizing influence of the large orbit ions is minimal. The highly kinetic ions were assumed to account for the observed stability of the FRC to several MHD instabilities, in particular the tilt instability [14,15]. The growth time, $1/\gamma_{\mathrm{tilt}}$ for this mode is $\sim l_s/2v_A = 0.015$ ms, where l_s is the axial FRC length. This time is not much less than the energy confinement time observed for the FRC formed initially, or after the RMF field is switched off. It is, however, many times too small to be consistent with the energy and particle confinement observed with the RMF present. The stabilizing influence of the RMF may likely be due to dynamic stabilization from the rapidly oscillating magnetic field pressure from the RMF antennas where $\omega_{\mathrm{RMF}} \gg \gamma_{\mathrm{tilt}}$. In fact, dynamic stabilization for this mode has been predicted theoretically [16,17]. For example, the oscillating antenna end currents (see Fig. 1) induce azimuthal currents at the end of the FRC that together with the steady radial magnetic field at the end of the FRC produce an axially oscillating force that drives a tiltlike perturbation. Crudely, for stability one would like $\omega_{\mathrm{RMF}}/\gamma_{\mathrm{tilt}}$ $(\sim 75) > B_z/B_\omega$ (~ 5) [17], so that stability can be achieved as long as the RMF field stays penetrated to the null.

The authors thank Dr. Richard Milroy and Dr. Alan Hoffman for many useful discussions, and Dr. Robert Brooks for help in data analysis. The ion temperature measurements were made by Dr. S. A. Cohen under a university support program from the Princeton Plasma Physics Laboratory.

[1] M. Tuszewski, Nucl. Fusion **28**, 2033 (1988).
[2] J. T. Slough *et al.,* Phys. Plasmas **2**, 2286 (1995).
[3] John Slough and Kenneth Miller, in Proceedings of the 35th AIAA/ASME/SAE/ASEE Joint Propulsion Conference, Los Angeles, 1999 (American Institute of Aeronautics and Astronautics, to be published), paper AIAA 99-2705.
[4] A. L. Hoffman and J. T. Slough, Nucl. Fusion **33**, 23 (1993).
[5] H. A. Blevin and P. C. Thonemann, Nucl. Fusion Suppl. **I**, 55 (1962).
[6] A. J. Knight and I. R. Jones, Plasma Phys. Controlled Fusion **32**, 575 (1990).
[7] I. R. Jones, Phys. Plasmas **6**, 1950 (1999).
[8] W. N. Hugrass, Aust. J. Phys. **38**, 157 (1985).
[9] R. D. Milroy, Phys. Plasmas **6**, 2771 (1999).
[10] R. D. Milroy, "A magnetohydrodynamic model of rotating magnetic field current drive in a field reversed configuration" (to be published).
[11] J. T. Slough, M. R. Kostora, D. E. Lotz, and K. E. Miller, Rev. Sci. Instrum. (to be published).
[12] J. T. Slough and K. E. Miller, Phys. Plasmas **7**, 1945 (2000).
[13] P. G. Carolan and V. A. Piotrowitz, Plasma Phys. **25**, 1065 (1983).
[14] M. N. Rosenbluth and M. N. Bussac, Nucl. Fusion **19**, 489 (1979).
[15] D. C. Barnes, J. L. Schwartzmeier, H. R. Lewis, and C. E. Seyler, Phys. Fluid **29**, 2616 (1986).
[16] W. K. Bertram, Aust. J. Phys. **42**, 379 (1989).
[17] S. A. Cohen, Bull. Am. Phys. Soc. **44**, 596 (1999).